Journal of Computational Physics 228 (2009) 5669–5686

Contents lists available at ScienceDirect

Journal of Computational Physics

journal homepage: www.elsevier.com/locate/jcp

A modified implicit Monte Carlo method for time-dependent radiative transfer with adaptive material coupling

Ryan G. McClarren [a,*], Todd J. Urbatsch [b]

[a] Institute for Applied Mathematics and Computational Science, Texas A&M University, College Station, TX 77843-3133, USA
[b] Computational Physics Group (CCS-2), Los Alamos National Laboratory, P.O. Box 1663, MS D409, Los Alamos, NM 87545, USA

ARTICLE INFO

Article history:
Received 8 December 2008
Received in revised form 13 April 2009
Accepted 15 April 2009
Available online 3 May 2009

Keywords:
Implicit Monte Carlo method
Thermal radiative transfer
High energy density physics

ABSTRACT

In this paper we develop a robust implicit Monte Carlo (IMC) algorithm based on more accurately updating the linearized equilibrium radiation energy density. The method does not introduce oscillations in the solution and has the same limit as $\Delta t \to \infty$ as the standard Fleck and Cummings IMC method. Moreover, the approach we introduce can be trivially added to current implementations of IMC by changing the definition of the Fleck factor. Using this new method we develop an adaptive scheme that uses either standard IMC or the modified method basing the adaptation on a zero-dimensional problem solved in each cell. Numerical results demonstrate that the new method can avoid the nonphysical overheating that occurs in standard IMC when the time step is large. The method also leads to decreased noise in the material temperature at the cost of a potential increase in the radiation temperature noise.

1. Introduction

Originally introduced by Fleck and Cummings [1], the implicit Monte Carlo (IMC) method is a stochastic means of solving the thermal radiative transfer equations. It manipulates the nonlinear equations describing thermal radiative transfer to get a linearized transport equation that can be solved using the standard Monte Carlo techniques for linear transport. Whereas the expected values of Monte Carlo tallies in linear transport can be exact, IMC has truncation error. These errors arise from the linearization of the material energy equation and from approximately time integrating the material energy equation. Also, spatial error is introduced by the necessity of having a spatial grid to describe the material temperature.

A particularly vexing problem with IMC is the potential for the solution to nonphysically violate the maximum principle that solutions to time-dependent radiative transfer obey [2]. This maximum principle states that if the material and radiation temperatures have initial and boundary data that lie within a temperature bounds, then the solution forever will lie between these bounds [3,4]. Both Larsen and Mercier [2] and Mosher and Densmore [5] have attempted to develop time step controls based on the infinite medium problem. The time step limits derived were prohibitively small and, for finite-dimensional problems, are more restrictive than necessary.

The violation of the maximum principle by IMC has been shown in infinite medium problems by Densmore and Larsen [6] where the material temperature becomes hotter than the maximum initial radiation temperature in one time step. On Marshak wave problems with a large time step, the IMC solution can have the material temperature higher than the boundary temperature [1]. A more subtle overheating phenomenon in IMC solutions occurs when, given initial data with the radiation temperature above the material temperature, the IMC solution nonphysically "flips" these temperatures [7].

* Corresponding author.
E-mail addresses: rgm@tamu.edu (R.G. McClarren), tmonster@lanl.gov (T.J. Urbatsch).

0021-9991/$ - see front matter © 2009 Elsevier Inc. All rights reserved.
doi:10.1016/j.jcp.2009.04.028

Various methods have attempted to correct certain errors in the IMC method. The Carter–Forest method [8] exactly solves the linearized material energy equation through a Monte Carlo procedure and the symbolic implicit Monte Carlo (SIMC) method [9,10] does not have linearization error but does introduce a time discretization error. Other recent work has defined a time-dependent Fleck factor (and source term) to more accurately treat the time dependence of the intensity over a time step [11].

Despite the potential benefits of other methods, IMC is the stochastic method used most often for simulating thermal radiative transfer. Below we derive a method that is similar to the Fleck and Cummings IMC method in that it represents the absorption/emission process through effective absorption and scattering, but differs in that it more accurately integrates the linearized material energy equation. This higher order method can be implemented in current IMC simulations simply by changing the definition of the Fleck factor. With the modified IMC method we devise an adaptive scheme to determine how much effective absorption or scattering there will be in the problem. This adaptive method takes the beginning of time step radiation and material temperatures in each cell and solves a zero-dimensional transport problem via standard IMC. If the material temperature in this 0-D solution is greater than the equilibrium temperature, the modified method is used to suppress this overheating.

2. Derivation for the gray case

We first will introduce the Fleck and Cummings [1] (IMC) method. After discussing this standard method, we will develop our new method.

2.1. Standard IMC method

We begin with the equations for grey thermal radiative transfer without scattering [1],

$$\frac{1}{c}\frac{\partial I}{\partial t}+\widehat{\Omega}\cdot\nabla I+\sigma I=\frac{1}{4\pi}\sigma acT^4, \tag{1a}$$

$$\frac{\partial u_{\mathrm{m}}}{\partial t}=\sigma\left(\int_{4\pi}Id\widehat{\Omega}-acT^4\right)+S. \tag{1b}$$

In these equations the specific intensity of radiation is denoted by $I(\mathbf{x},\widehat{\Omega},t)$, T is the material temperature, u_{m} is the material energy density, $\widehat{\Omega}$ is the direction of flight, a is the radiation constant, c is the speed of light, S is an arbitrary source function and $\sigma(x,T)$ is the opacity of the material and has units of inverse length. Eq. (1a) models the transport of the radiation through the material medium and Eq. (1b) governs the change in material energy from the source S and radiation being absorbed and emitted by the material.

To derive an implicit Monte Carlo method for these equations we will define the equilibrium energy density variable as

$$u_{\mathrm{r}}=aT^4. \tag{2}$$

In words, u_{r} is the value of the radiation energy density when the material and radiation are in equilibrium. As is standard, we also write

$$\frac{\partial u_{\mathrm{m}}}{\partial u_{\mathrm{r}}}=\beta^{-1}. \tag{3}$$

In the simple case of constant specific heat, c_{v}, where the material energy density is given by $u_{\mathrm{m}}=\rho c_{\mathrm{v}}T$, we have $\beta=\frac{4aT^3}{\rho c_{\mathrm{v}}}$. Using our newly defined variables we can rewrite Eq. (1) as

$$\frac{1}{c}\frac{\partial I}{\partial t}+\widehat{\Omega}\cdot\nabla I+\sigma I=\frac{1}{4\pi}c\sigma u_{\mathrm{r}}, \tag{4a}$$

$$\frac{\partial u_{\mathrm{r}}}{\partial t}=\beta\sigma\left(\int_{4\pi}Id\widehat{\Omega}-cu_{\mathrm{r}}\right)+\beta S. \tag{4b}$$

The goal of an implicit Monte Carlo method is to get an implicit definition of u_{r} from Eq. (4b) to linearize Eq. (4a) allowing for a Monte Carlo solution of the radiation transport equation.

The Fleck and Cummings procedure averages Eq. (4b) over a time step as

$$\frac{u_{\mathrm{r}}^{n+1}-u_{\mathrm{r}}^{n}}{\Delta t}=\frac{1}{\Delta t}\int_{t_n}^{t_{n+1}}dt\left[\beta\sigma\left(\int_{4\pi}Id\widehat{\Omega}-cu_{\mathrm{r}}\right)+\beta S\right], \tag{5}$$

where the superscripts denote the time level. Then the average value of u_{r} is written as an interpolation between the beginning and end of step values

$$\tilde{u}_r\equiv\frac{1}{\Delta t}\int_{t_n}^{t_{n+1}}dtu_{\mathrm{r}}\approx\alpha u_{\mathrm{r}}^{n+1}+(1-\alpha)u_{\mathrm{r}}^{n}. \tag{6}$$

Using the definition of $\tilde{u}_r$ in Eq. (5) gives

$$u_r^{n+1} = u_r^n + \int_{t_n}^{t_{n+1}} dt \beta\sigma \int_{4\pi} I d\hat{\Omega} - c\Delta t \overline{\beta\sigma}(\alpha u_r^{n+1} + (1-\alpha)u_r^n) + \Delta t \overline{\beta S}, \tag{7}$$

where $(\cdot)$ denotes a properly time-averaged quantity, $\alpha \in [\frac{1}{2}, 1]$ is the implicitness factor and the superscripts denote the time level. In practice α is almost always set to unity because smaller values of α can lead to oscillatory behavior in the solution although $\alpha = 1/2$ gives a second-order update when β and σ are constant. Also, $\overline{\beta\sigma}$ are generally evaluated at the n time level as $\beta^n\sigma^n$ and a similar approximation is made for $\overline{\beta S}$. A consistent approximation to Eq. (7) is [6]

$$u_r^{n+1} = u_r^n + \Delta t \overline{\beta\sigma} \int_{4\pi} I d\hat{\Omega} - c\Delta t \overline{\beta\sigma}(\alpha u_r^{n+1} + (1-\alpha)u_r^n) + \Delta t \overline{\beta S}, \tag{8}$$

where the error in this approximation is $O(\Delta t)$. This approximation is consistent in the sense that as $\Delta t \to 0$, Eqs. (7) and (8) are identical.

Eq. (8) can be rewritten as

$$\tilde{u_r} = f u_r^n + \frac{(1-f)}{c}\left(\int_{4\pi} I d\hat{\Omega} + \frac{1}{\sigma} S\right), \tag{9}$$

with

$$f = \frac{1}{1 + \alpha\beta\sigma c\Delta t}, \tag{10}$$

and for convenience we have dropped the overbars from β, S, and σ. The expression for $\tilde{u}_r$ from Eq. (9) is then substituted into the transport equation, Eq. (4a), to get the linear transport equation to be solved by Monte Carlo:

$$\frac{1}{c}\frac{\partial I}{\partial t} + \hat{\Omega}\cdot\nabla I + \sigma I = \frac{1}{4\pi}(1-f)\sigma \int_{4\pi} I d\hat{\Omega} + \frac{1}{4\pi}(c\sigma f u_r + (1-f)S). \tag{11}$$

This transport equation has some interesting properties. As a result of the procedure for determining $\tilde{u}_r$, Eq. (11) has effective scattering and absorption coefficients given by

$$\sigma_s = (1-f)\sigma, \quad \sigma_a = f\sigma. \tag{12}$$

Eq. (11) can be solved with a standard linear Monte Carlo solution technique. We also note that the factor f is bounded by $0 \leqslant f \leqslant 1$ and that as $\Delta t \to \infty$ the value of f goes to zero, which is to say that, in the limit of an infinite time step, there is no effective absorption and the material energy will not change over a time step.

Before continuing, we want to point out that the material energy and temperature are not updated based on Eq. (8). Rather the change in material energy is computed at the end of time step by tallying the number of absorption and emission events in a particular cell during a timestep:

$$\Delta u_m = \sum_{i=0}^{\#\,\text{absorptions}} (h\nu)_i - \sum_{j=0}^{\#\,\text{emissions}} (h\nu)_j, \tag{13}$$

where $(h\nu)_i$ is the energy of the photon involved in event i. Nonetheless, for 0-D problems it is possible to give a solution for the change of material energy during a time step in the limit of infinite particles [5],

$$\Delta u_m = \left(\frac{1}{c}\int_{4\pi} I^n d\hat{\Omega} - u_r^n\right)(1 - e^{-fc\sigma^n\Delta t}). \tag{14}$$

We will revisit this expression below when we develop an adaptive update scheme.

2.1.1. Approximations in IMC

We now briefly summarize the approximations in the Fleck and Cummings procedure. First, we note that the material energy equation was linearized by approximating the value of β and σ with a single value; in reality these values change nonlinearly with the material energy. This approximation is hard to avoid because we generally desire a linear transport equation to solve via Monte Carlo. It would be possible to define an iterative procedure to remove the linearization error by linearizing Eq. (1b) and solving a linear transport equation in each iteration. Such a iterative method is prohibitively expensive because it would involve several Monte Carlo solutions per time step. The linearization error is also addressed by the symbolic implicit Monte Carlo method (SIMC) [9,10] where Eq. (1b) is not linearized but σ is evaluated at the previous time step value.

The other main approximation in the Fleck and Cummings IMC method is that the instantaneous intensity, I, is used in the definition of u_r^{n+1} in going from Eqs. (7) to (8), which is equivalent to assuming that the time dependence of I does not influence the emission process. Under this assumption the re-emission process is instantaneous and is modeled by effective scattering. Moreover, with the approximation that the time dependence of I does not affect the emission, the strength of the emission source cannot change over the time step. The Carter–Forest method [8] addresses this issue by defining time-dependent source and re-emission terms that are sampled in the Monte Carlo solution of the transport equation. Also, other recent work has defined a time-dependent Fleck factor that tunes the parameter α to achieve a more accurate solution [11].

2.2. High-order update for u_r^{n+1}

Despite its shortcomings, the Fleck and Cummings IMC method is widely used to solve time-dependent radiative transfer problems. In this study we do not address the approximations in IMC discussed above (linearization and instantaneous absorption/emission). Rather, we will address the temporal truncation error in the IMC method.

The value of u_r^{n+1} given by Eq. (9) is a first-order in Δt approximation to the solution of Eq. (4b). The method we introduce in this study hinges on the fact that it is possible to exactly integrate Eq. (4b) using an integrating factor under the assumptions that β, σ and S are constant.

The exact solution of Eq. (4b) at time t_{n+1}, when β and σ are approximated by a single value, is given by

$$u_r^{n+1} = e^{-\beta\sigma c\Delta t}u_r^n + e^{-\beta\sigma c\Delta t}\beta\sigma\int_{t_n}^{t_{n+1}} dt\, e^{\beta\sigma c(t-t_n)}\int_{4\pi} Id\widehat{\Omega} + \frac{1-e^{-\beta\sigma c\Delta t}}{c\sigma}S. \tag{15}$$

We note that Eq. (15) is equivalent to the time-dependent source and emission terms that the Carter–Forest method simulates via a Monte Carlo procedure. Rather than solve the Carter–Forest equations, we make a consistent approximation by writing

$$\int_{t_n}^{t_{n+1}} dt\, e^{\beta\sigma c(t-t_n)}I(t) \approx \frac{1}{\beta\sigma c}(e^{\beta\sigma c\Delta t}-1)I(t), \tag{16}$$

thereby incurring an $O(\Delta t)$ error to get

$$u_r^{n+1} = e^{-\beta\sigma c\Delta t}u_r^n + \frac{1}{c}(1-e^{-\beta\sigma c\Delta t})\left(\int_{4\pi} Id\widehat{\Omega} + \frac{1}{\sigma}S\right), \tag{17}$$

or more compactly

$$u_r^{n+1} = m_\infty u_r^n + \frac{1}{c}(1-m_\infty)\left(\int_{4\pi} Id\widehat{\Omega} + \frac{1}{\sigma}S\right), \tag{18}$$

with

$$m_\infty = e^{-\beta\sigma c\Delta t}. \tag{19}$$

As in the Fleck and Cummings method we have introduced an $O(\Delta t)$ error in going from Eqs. (15) to (17).

Substituting the value of u_r^{n+1} given by Eq. (18) into the transport equation we get

$$\frac{1}{c}\frac{\partial I}{\partial t} + \widehat{\Omega}\cdot\nabla I + \sigma I = \frac{1}{4\pi}(1-m_\infty)\sigma\int_{4\pi} Id\widehat{\Omega} + \frac{1}{4\pi}(c\sigma m_\infty u_r + (1-m_\infty)S). \tag{20}$$

Note that the only difference in using the exact update for u_r^{n+1} is changing $f \to m_\infty$. We have the same definitions for the effective scattering and absorption, only evaluated with m_∞. The range and limits of m_∞ are the same as f; m_∞ is in $[0,1]$ and limits to zero as $\Delta t \to \infty$.

3. Properties of m_∞

As noted above, the Fleck and Cummings method gives a first-order in Δt update of u_r^{n+1} when $\alpha = 1$. This can be shown by a Taylor expansion of f about $\Delta t = 0$

$$f = 1 - \beta\sigma c\Delta t + (\beta\sigma c\Delta t)^2 + O(\Delta t^3). \tag{21}$$

The same Taylor series for m_∞ is

$$m_\infty = 1 - \beta\sigma c\Delta t + \frac{1}{2}(\beta\sigma c\Delta t)^2 + O(\Delta t^3). \tag{22}$$

Comparing terms in these series we see that f approximates m_∞ to $O(\Delta t^2)$. This indicates that the Fleck and Cummings update for u_r^{n+1} is first-order in Δt when β and σ are constant over the time step. The method is first-order because the convergence rate for a time-integration method is one order less than the order of the error for one time step due to the fact that error accumulates over several time steps [12].

The total error in a Fleck and Cummings time step is $\beta\sigma c O(\Delta t^2) + O(\Delta t)\int_{4\pi} Id\widehat{\Omega}$ because of the approximation made in the time dependence of I. When f is replaced by m_∞ the error in one step is $O(\Delta t)\int_{4\pi} Id\widehat{\Omega}$.

As our numerical results will demonstrate, the factor m_∞ may cause the material temperature to change negligibly when large time steps are used. At large values of $\beta\sigma c\Delta t$ the linearization error in IMC is large. For large $\beta\sigma c\Delta t$ the change in u_r over a time step is negligibly small when m_∞ is used. The errors introduced by f allow u_r to change over a time step when $\beta\sigma c\Delta t$ is large. Of course it is possible that too much heating is allowed, producing nonphysical material temperatures. Our numerical results will show that m_∞ gives too little material heating and it is necessary to use a different factor than m_∞ for large time steps.

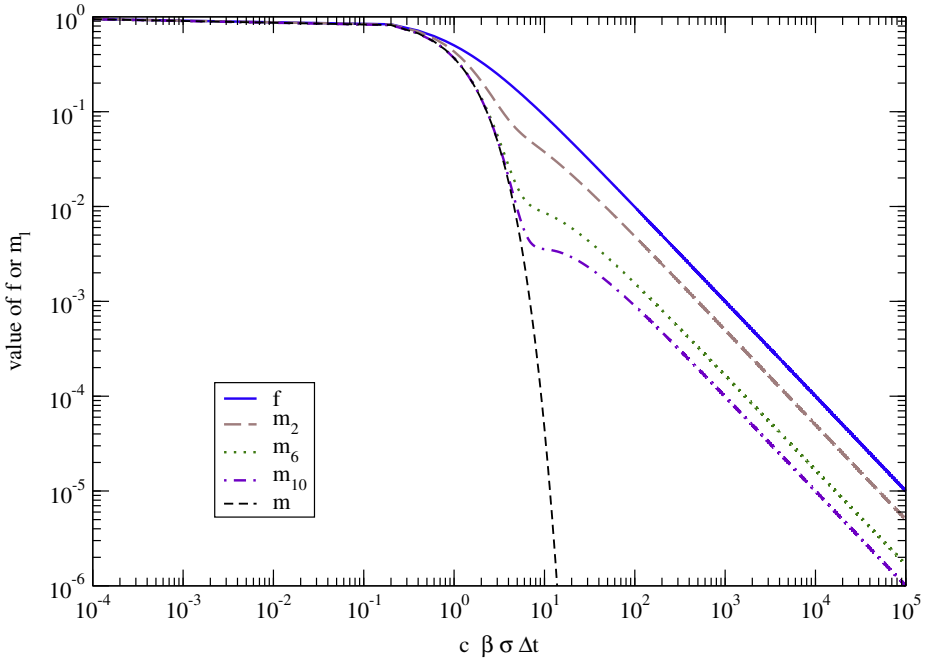

Fig. 1. A comparison of the Fleck factor, f_0 and the m factor from the modified IMC method.

A reason that m_∞ can allow too little heating compared with f is that at large values of $\beta\sigma c\Delta t$, m_∞ decays exponentially, rather than the rational polynomial decay of f. Therefore, we desire to construct an approximation to m_∞ that at some point begins to decay rationally when $\beta\sigma c\Delta t$ is above some threshold. One way of constructing an approximation to m_∞ that transitions to rational polynomial behavior is

$$m_l \equiv e^{-\beta\sigma c\Delta t} + \frac{1}{l}\frac{(\beta\sigma c\Delta t)^l}{(1+\beta\sigma c\Delta t)^{l+1}}. \tag{23}$$

Each m_l, for l an integer, gives an lth order approximation to m_∞. We demonstrate this point by noting that

$$\frac{1}{l}\frac{(\beta\sigma c\Delta t)^l}{(1+\beta\sigma c\Delta t)^{l+1}} = O(\Delta t^l); \tag{24}$$

that is, the rational expression in the definition of m_l adds an order l error. We use the above formulation rather than a Taylor series approximation because a Taylor series would not have the exponential behavior for intermediate values of $\beta\sigma c\Delta t$ and it takes many terms to make a Taylor series expansion of m_∞ significantly different than f.

Notice that the only difference between our IMC method and the Fleck and Cummings IMC method is in the difference between f and m_l. If these two factors were identical then our method would give the same result as standard IMC. The difference between f and m are presented in Fig. 1. Since $f \leqslant m_l$, our modified IMC method always has more effective scattering than standard IMC when the time step is large compared to the time scale of the absorption/emission process.

Fig. 1 also shows how the m_l values differ from m_∞ and f. The l value determines at which value of $\beta\sigma c\Delta t$ the m_l approximation breaks away from m_∞ and begins to decay with rational polynomial behavior. For higher values of l, m_l matches m_∞ to larger values of $\beta\sigma c\Delta t$. After breaking away from the exponential curve of m_∞, m_l goes as $(\beta\sigma c\Delta t)^{-1}$, the same behavior as f.

As we shall see in our numerical results, in problems where the opacity is a function of the temperature, the smaller amount of heating in the m_l solutions can affect the evolution of the system, even when standard IMC does not cause overheating. In these cases it would be possible to use the standard f factor when $\beta\sigma c\Delta t$ is small and overheating is not an issue and use m_l for an appropriate value of l when $\beta\sigma c\Delta t$ is large. We shall use these ideas to develop an adaptive method where l is chosen dynamically.

4. Equilibrium diffusion limit analysis

The equilibrium diffusion limit of the thermal radiative transfer system, Eq. (4), occurs when the opacity, σ, is large compared to the length scale on which I and u_m vary and when the time dependence of I and u_m and the source S are small

compared to that same length scale (this in turn makes β large) [6,13]. The equilibrium diffusion limit can be arrived at by defining a small, positive parameter ϵ and scaling Eq. (4) as

$$\frac{\epsilon}{c}\frac{\partial I}{\partial t}+\widehat{\Omega}\cdot\nabla I+\frac{1}{\epsilon}\sigma I=\frac{1}{4\pi\epsilon}c\sigma u_r, \tag{25a}$$

$$\frac{\partial u_r}{\partial t}=\frac{1}{\epsilon^2}\beta\sigma\left(\int_{4\pi} Id\widehat{\Omega}-cu_r\right)+\beta S. \tag{25b}$$

and taking the limit as $\epsilon\to 0$ away from boundary and initial layers. This limit [13] gives the leading order intensity as a Planckian at the local temperature,

$$I^{(0)}=\frac{1}{4\pi}ac(T^{(0)})^4, \tag{26}$$

where the superscript (0) denotes terms that are zeroth order in ϵ. The leading order temperature satisfies the nonlinear diffusion equation,

$$\frac{\partial}{\partial t}u_m(T^{(0)})+a\frac{\partial}{\partial t}(T^{(0)})^4=\nabla\cdot\frac{ac}{3\sigma}\nabla(T^{(0)})^4, \tag{27}$$

and the first moment in $\widehat{\Omega}$ of the radiation intensity (generally called the radiation flux) is an order ϵ quantity given by

$$\left(\int_{4\pi}\widehat{\Omega}Id\widehat{\Omega}\right)^{(1)}=\frac{ac}{3\sigma}\nabla(T^{(0)})^4. \tag{28}$$

To examine how our IMC method behaves in this limit we first look at m_l under the scaling $\sigma\to\sigma/\epsilon$,

$$m_l\to\frac{\epsilon^2}{l\beta\sigma c\Delta t}+O(\epsilon^4). \tag{29}$$

That is, m_l is an $O(\epsilon^2)$ quantity. This implies that the effective scattering will be σ to leading order and that the effective absorption will be an order ϵ^2 quantity. In their analysis of the Fleck and Cummings IMC method, Densmore and Larsen [6] found the same scaling for the effective scattering and absorption. Therefore, their results for the equilibrium diffusion limit of the Fleck and Cummings method applies to our method as well.

Using the results of Densmore and Larsen, in the equilibrium diffusion limit our method solves the following diffusion equation

$$\frac{u_m(T^{(0)}_{n+1})-u_m(T^{(0)}_n)}{\Delta t}+\frac{1}{c}\frac{\phi^{(0)}_{n+1}-\phi^{(0)}_n}{\Delta t}=\frac{1}{\Delta t}\int_{t^n}^{t^{n+1}}dt\,\nabla\cdot\frac{1}{3\sigma}\nabla\phi^{(0)}, \tag{30}$$

where

$$\phi=\int_{4\pi}d\widehat{\Omega}I, \tag{31}$$

and we have used subscripts to indicate time level. This equation is similar to Eq. (27) except that it does not enforce the equilibrium between ϕ and acT^4. This shortcoming of standard IMC in the equilibrium diffusion limit is not corrected by using a higher order approximation to u_r. Nevertheless, we know that the two methods will behave similarly in this limit.

5. Frequency dependent case

The frequency dependent case poses no particular problems for developing a high order implicit Monte Carlo method. In this case the equations we wish to solve are

$$\frac{1}{c}\frac{\partial I_\nu}{\partial t}+\widehat{\Omega}\cdot\nabla I_\nu+\sigma_\nu I_\nu=\frac{1}{4\pi}c\sigma_\nu b_\nu u_r, \tag{32a}$$

$$\frac{\partial u_r}{\partial t}=\beta\left(\int_0^\infty d\nu\int_{4\pi}d\widehat{\Omega}\sigma_\nu I_\nu-c\sigma_p u_r\right)+\beta S, \tag{32b}$$

where $I_\nu(x,\widehat{\Omega},\nu,t)$ is the frequency dependent specific intensity and b_ν is the normalized Planck spectrum defined by

$$b_\nu=\frac{B_\nu}{u_r}, \tag{33}$$

where the frequency dependent Planck function is

$$B_\nu=\frac{2h\nu^3}{c^2}(e^{h\nu/kT}-1)^{-1}, \tag{34}$$

with h and k the Planck and Boltzmann constants respectively. We have also defined the frequency dependent opacity σ_ν and the Planck averaged absorption opacity as

$$\sigma_{\mathrm{p}} = \int_0^\infty b_\nu \sigma_\nu d\nu. \tag{35}$$

We integrate Eq. (32b) as in the grey case to write

$$u_{\mathrm{r}}^{n+1} = m_\infty u_{\mathrm{r}}^n + \frac{(1-m_\infty)}{c\sigma_{\mathrm{p}}}\left(\int_0^\infty d\nu \int_{4\pi} d\widehat{\Omega}\sigma_\nu I_\nu + S\right) \tag{36}$$

where

$$m_\infty = e^{-\beta\sigma_{\mathrm{p}} c\Delta t}. \tag{37}$$

Upon substituting u_{r}^{n+1} from Eq. (36) into Eq. (32a) we get the linear transport equation

$$\frac{1}{c}\frac{\partial I_\nu}{\partial t} + \widehat{\Omega}\cdot\nabla I_\nu + \sigma_\nu I_\nu = \frac{1}{4\pi}\frac{\sigma_\nu b_\nu}{\sigma_{\mathrm{p}}}(1-m_\infty)\int_0^\infty d\nu' \int_{4\pi} d\widehat{\Omega}'\sigma'_\nu I'_\nu + \frac{cm\sigma_\nu b_\nu}{4\pi}u_{\mathrm{r}}^n + \frac{1}{4\pi}\frac{\sigma_\nu b_\nu}{\sigma_{\mathrm{p}}}(1-m_\infty)S. \tag{38}$$

In this equation the effective differential scattering cross-section is

$$\frac{d^2\sigma}{d\widehat{\Omega}d\nu}(\nu'\to\nu) = \frac{1}{4\pi}\sigma'_\nu\frac{\sigma_\nu b_\nu}{\sigma_{\mathrm{p}}}(1-m_\infty). \tag{39}$$

The total effective scattering and absorption cross-sections are given by integrating Eq. (38) over $\widehat{\Omega}$ and ν to get

$$\sigma'_{\nu s} = (1-m_\infty)\sigma'_\nu, \tag{40}$$

$$\sigma'_{\nu a} = m_\infty\sigma'_\nu. \tag{41}$$

Similarly to Eq. (23) we can define an approximation to m_∞

$$m_l = e^{-\beta\sigma_{\mathrm{p}} c\Delta t} + \frac{1}{l}\frac{(\beta\sigma_{\mathrm{p}} c\Delta t)^l}{(1+\beta\sigma_{\mathrm{p}} c\Delta t)^{l+1}}. \tag{42}$$

Eq. (38) compares with the Fleck and Cummings IMC method for multifrequency problems where the transport equation solved is

$$\frac{1}{c}\frac{\partial I_\nu}{\partial t} + \widehat{\Omega}\cdot\nabla I_\nu + \sigma_\nu I_\nu = \frac{1}{4\pi}\frac{\sigma_\nu b_\nu}{\sigma_{\mathrm{p}}}(1-f)\int_0^\infty d\nu' \int_{4\pi} d\widehat{\Omega}'\sigma'_\nu I'_\nu + \frac{cf\sigma_\nu b_\nu}{4\pi}u_{\mathrm{r}}^n + \frac{1}{4\pi}\frac{\sigma_\nu b_\nu}{\sigma_{\mathrm{p}}}(1-f)S, \tag{43}$$

where

$$f = \frac{1}{1+\beta\sigma_{\mathrm{p}} c\Delta t}. \tag{44}$$

As in the grey case, the only difference between Fleck and Cummings IMC and our method is the factors f and m_l.

6. Comparison on 0-D problems

We now compare methods using an infinite medium problem first explored by Densmore and Larsen [6]. In this problem there is a temperature-independent opacity of $\sigma = 100\,\mathrm{cm}^{-1}$ and a temperature-independent heat capacity of $\rho c_v = 0.01\,\mathrm{GJ/cm^3\text{-}keV}$ (1 GJ = 1 gigajoule = 10^9 J) and an initial material temperature of $T = 0.4$ keV. For units of time we use the nanosecond (10^{-9} s) and keV for temperature. Expressing physical constants in these units gives the speed of light, c, as 29.98 cm/ns and the radiation constant, a, as $0.01372\,\mathrm{GJ/cm^3\text{-}keV^4}$. For this problem, the mean-free time of a photon, $(c\sigma)^{-1}$, is 3.34×10^{-4} ns. The Fleck and Cummings results we obtain for this problem mirror those obtained by Densmore and Larsen. We also compare the numerical methods with the exact solution for this problem, as given by Mosher [14]. The code used to compute Mosher's result was contributed by Gentile [15].

In Figs. 2 through 5 the problem has the initial material temperature given by $T = 0.4$ keV and the initial radiation temperature as $T_{\mathrm{R}} = 0.5$ keV, where

$$T_{\mathrm{R}} = \sqrt[4]{\frac{\phi}{ac}}. \tag{45}$$

Fig. 2 gives results obtained with a time step of $\Delta t = 0.01$ ns. In this figure, the time step size is much larger than the mean-free time, therefore we desire that the numerical results go to the equilibrium value of the material and radiation temperatures after one time step. As expected for such an optically long time step, the exact solution has reached equilibrium well before the end of the first time step. Indeed it is asking a lot for a numerical method to capture the steep transient that is present in the exact solution in one time step. For the numerical results, at one extreme, the Fleck and Cummings solution,

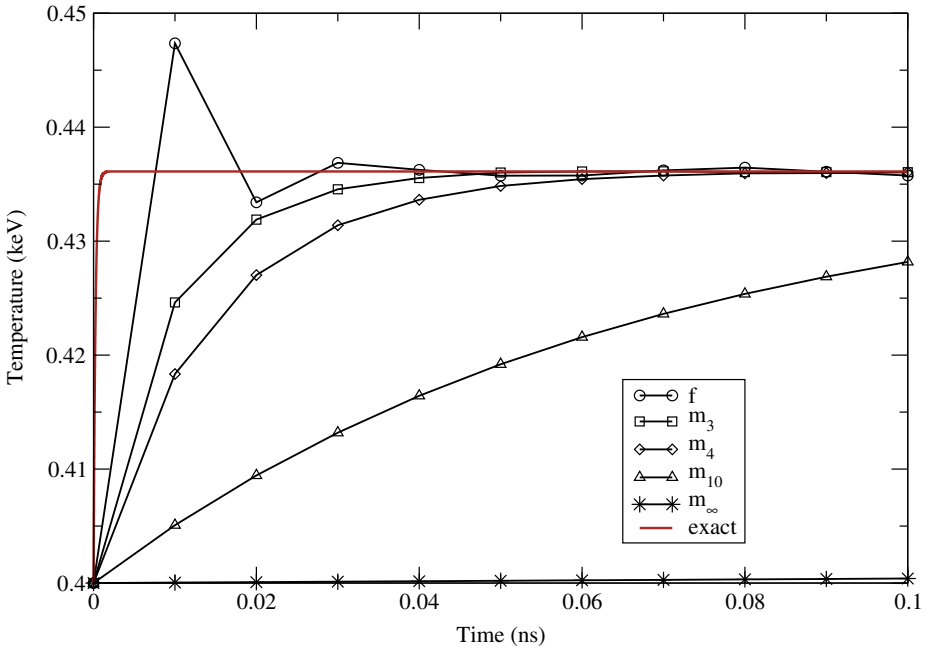

Fig. 2. Infinite medium material temperature with initial $T_R = 0.5$ keV, $\Delta t = 0.01$ ns for different factors, either f or m_l.

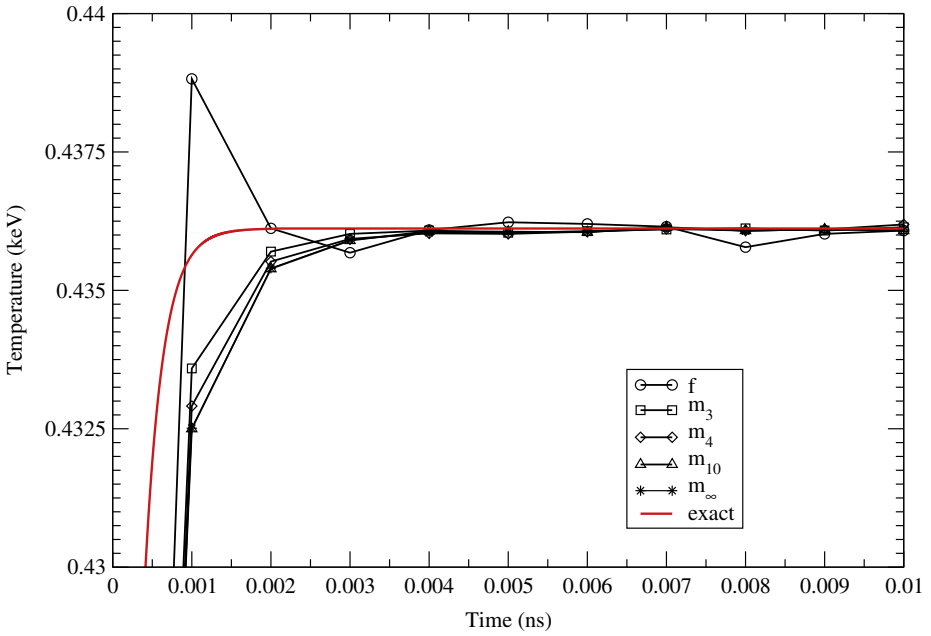

Fig. 3. Infinite medium material temperature with initial $T_R = 0.5$ keV, $\Delta t = 0.001$ ns.

denoted in the figure by f, has the material temperature exceeding the equilibrium temperature after one time step. Successive time steps have the Fleck and Cummings solution nonphysically oscillating about the equilibrium value. These results for Fleck and Cummings indicate that it is allowing too much absorption in the first time step, causing the material to heat up too much. At the other extreme, the m_∞ solution only slightly heats up over the entire simulation time. For m_∞ there is too much effective scattering so there is no heating in the problem. The m_{10} solution is similar to the m_∞ solution in that there is not enough heating and the solution does not reach the equilibrium solution in the simulated time. The m_3 and m_4 solutions do not overshoot the equilibrium value and approach the equilibrium solution monotonically from below, but they do not reach equilibrium in one time step.

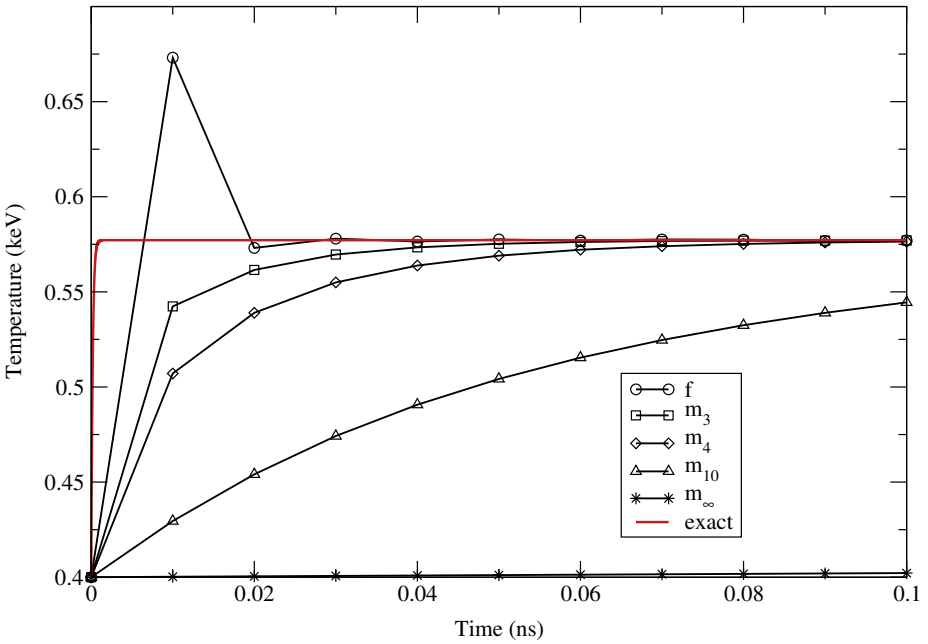

Fig. 4. Infinite medium material temperature with initial $T_{\mathrm{R}} = 0.7$ keV, $\Delta t = 0.01$ ns.

The consequences of decreasing the time step are shown in Fig. 3. Here the time step is $\Delta t = 0.001$ ns and $T_{\mathrm{R}} = 0.5$ keV. This time step is still several mean-free times long and at $t = 0.001$ ns the exact solution is nearly in equilibrium. The Fleck and Cummings solution still overshoots the equilibrium temperature in the first time step and oscillates about the equilibrium thereafter. All of the m_l solutions, including the m_∞ solution, approach the equilibrium solution from below and reach the equilibrium solution monotonically from below.

Overheating of the material temperature can cause problems in a coupled radiation hydrodynamics simulation. In such a calculation if the material temperature nonphysically overheats, as in the Fleck and Cummings solutions under discussion, the hydrodynamic solution will incorrectly evolve because of the too large amount of energy deposited in the material by the radiation.

Fig. 4 shows results where the initial values of T_{R} and T are farther out of equilibrium, $T_{\mathrm{R}} = 0.7$ keV and as before the exact solution reaches equilibrium before the end of one time step. In this problem the Fleck and Cummings solution overshoots the equilibrium value by about 17% and then oscillates about the equilibrium solution. The m_3 and m_4 solutions give a solution below the equilibrium value and take several time steps to reach the equilibrium. The m_{10} and m_∞ solutions never reach the equilibrium value in the length of time simulated.

Results for a large disparity in the initial material and radiation temperature are shown in Fig. 5. Here $T_{\mathrm{R}} = 1.0$ keV. In this figure the Fleck and Cummings solution overshoots the equilibrium value by about 100% and does not get near the equilibrium value until the fourth time step. The m_3 solution also overheats in the first time step and then cools to the equilibrium solution. However, compared to the Fleck and Cummings solution it takes longer for the m_3 solution to reach the equilibrium temperature. The m_4 solution is within 1% of the equilibrium solution in the first time step. Finally, the m_{10} and m_∞ solutions underpredict the material temperature.

7. Adaptive method for choosing *l*

The 0-D results presented above show the benefits to the modified method and the drawbacks to standard IMC. The question of how to pick l is still open; in the 0-D cases, no single selection of l was ideal for every problem. However, we can *a priori* decide which l will work best for a given infinite medium problem. This decision is based on constraining the end of time step material temperature to be less than the equilibrium temperature, if it starts out less than the equilibrium temperature.

To choose the appropriate value of l we first determine if $T_{\mathrm{R}} > T$. If so, then the material temperature could overshoot the equilibrium temperature. If $T > T_{\mathrm{R}}$, then material overheating cannot occur and we can use standard IMC. When $T_{\mathrm{R}} > T$, we then determine if this overshoot occurs by solving a 0-D problem. For a 0-D problem, IMC has the solution for the material energy given by Eq. (14) [5]

$$\Delta u_{\mathrm{m}} = \left(a(T_{\mathrm{R}}^n)^4 - u_{\mathrm{r}}^n\right)[1 - e^{-f\sigma c\Delta t}], \tag{46}$$

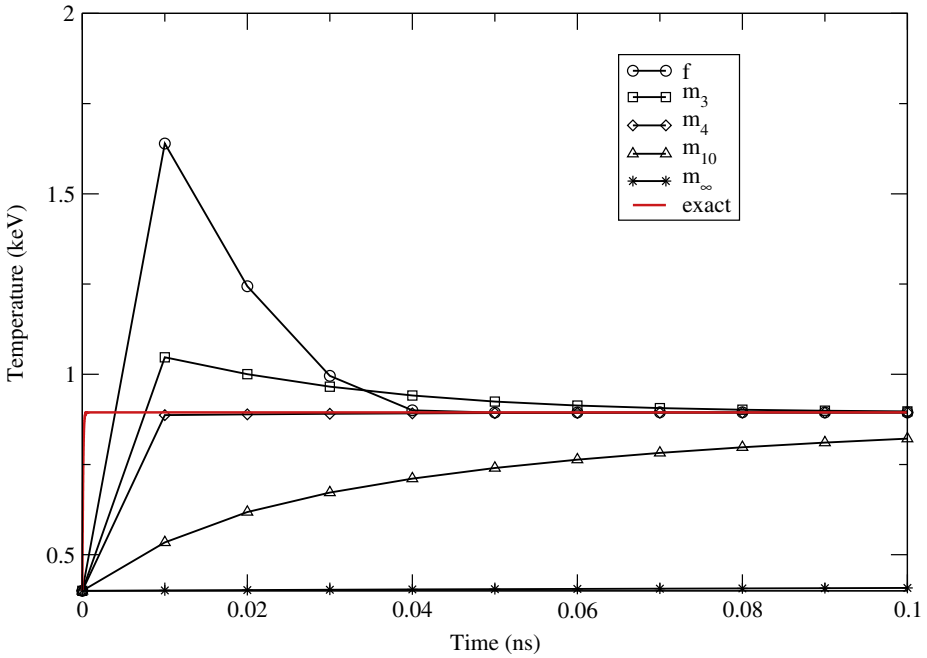

Fig. 5. Infinite medium material temperature with initial $T_{\mathrm{R}} = 1.0$ keV, $\Delta t = 0.01$ ns.

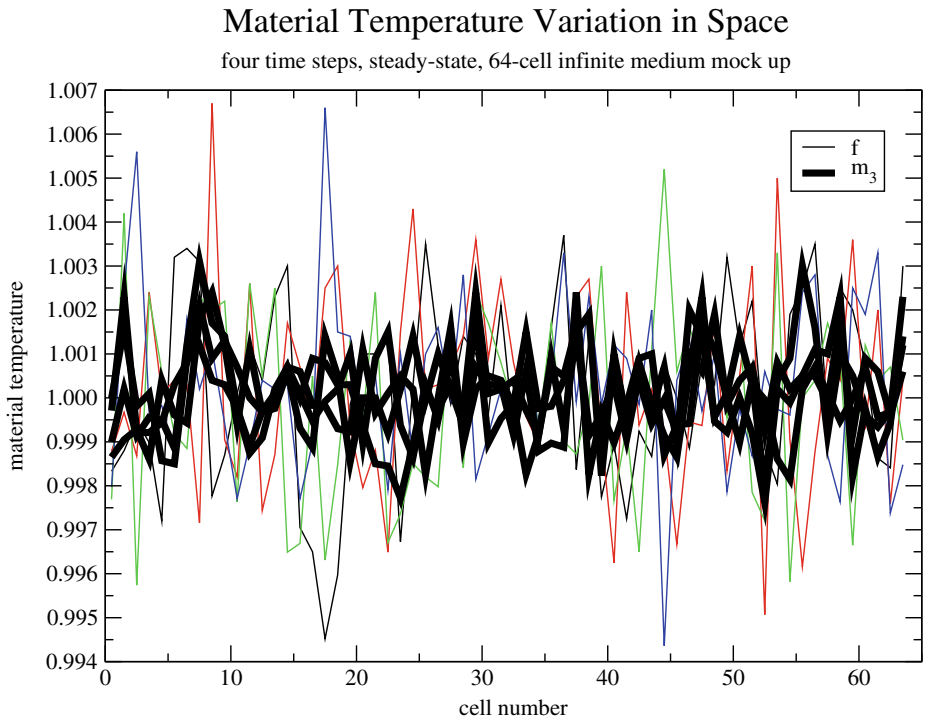

Fig. 6. Comparison of material temperatures at four different time steps from standard IMC and our adaptive method. The analytic solution to this problem is a constant material temperature of 1 keV for each cell and the thicker lines for the m_3 solution show a smaller variance than the f solution.

From Δu_{m} we can calculate u_{m}^{n+1} and determine T_{n+1} via the equation of state. This is compared with the equilibrium temperature. The equilibrium temperature, T_{eq} is found by solving an expression of the conservation of total (radiation and material) energy:

$$a(T_{\mathrm{R}}^{n})^4 + u_{\mathrm{m}}^{n} = aT_{\mathrm{eq}}^4 + u_{\mathrm{m}}(T_{\mathrm{eq}}). \tag{47}$$

If T_{n+1} is greater than T_{eq}, then we recompute T_{n+1} using m_2 instead of f. If m_2 overshoots the equilibrium temperature, then we increase l until $T_{n+1} \leqslant T_{\mathrm{eq}}$.

We use a similar procedure for multidimensional problems. In this case we solve a 0-D problem in each computational cell. The 0-D problem we solve has the radiation temperature given as the maximum of the radiation temperature in the cell and the temperatures (both radiation and material) in its neighboring cells. This takes into account the fact that energy can move between cells. Using data from neighboring cells should be effective when the cells are optically thick. It is precisely in the case of optically thick cells that overheating can be a problem; cells containing few mean-free paths will most likely not have too much absorption in a time step because radiation from neighboring cells will stream through such an optically thin cell. Also, for multidimensional problems we set a problem-dependent maximum value for l. We allow such a maximum because the 0-D solution can be too restrictive in suppressing material heating and force l to be larger than needed for multidimensional problems.

Henceforth, when we refer to a numerical solution as the m_l solution we are referring to the adaptive method with the maximum value of l in computing the integration factor m_l.

8. Figure of Merit for adaptive method

The goal of this new method is to mitigate the nonphysical overheating that occurs with the standard Fleck and Cummings IMC method. It does this by increasing the effective scattering and decreasing the effective absorption. A consequence of this method is potentially reduced statistical noise in the material temperature. When there is less absorption, there is less effective emission and the material and radiation tend to become increasingly decoupled. Thus, the material tends to remain unchanged and therefore its temperature may display less statistical noise. The benefit of this reduced noise comes at the cost of increased computational run times due to longer particle lifetimes with more scattering. We are thus motivated to determine a quantitative measure of this noise reduction. The standard Figure of Merit (FOM) was developed to compare variance reduction techniques in linear Monte Carlo transport [16]. We can apply the FOM to time-dependent, nonlinear calculations if we compare identical snapshots of the two different methods on the same computer. We will use the following FOM expression,

$$\mathrm{FOM} = \frac{1}{\sigma^2 t}, \tag{48}$$

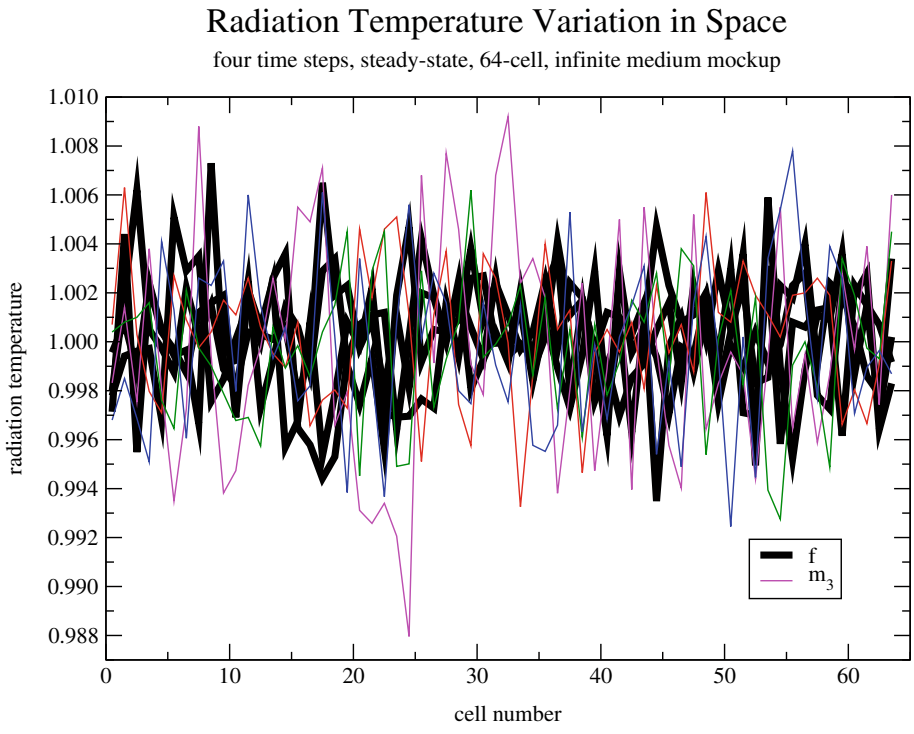

Fig. 7. Comparison of radiation temperatures at four different time steps from standard IMC and our adaptive method. This plot is similar to Fig. 6 except the thicker lines for the f solution show less variance than the m_3 solution.

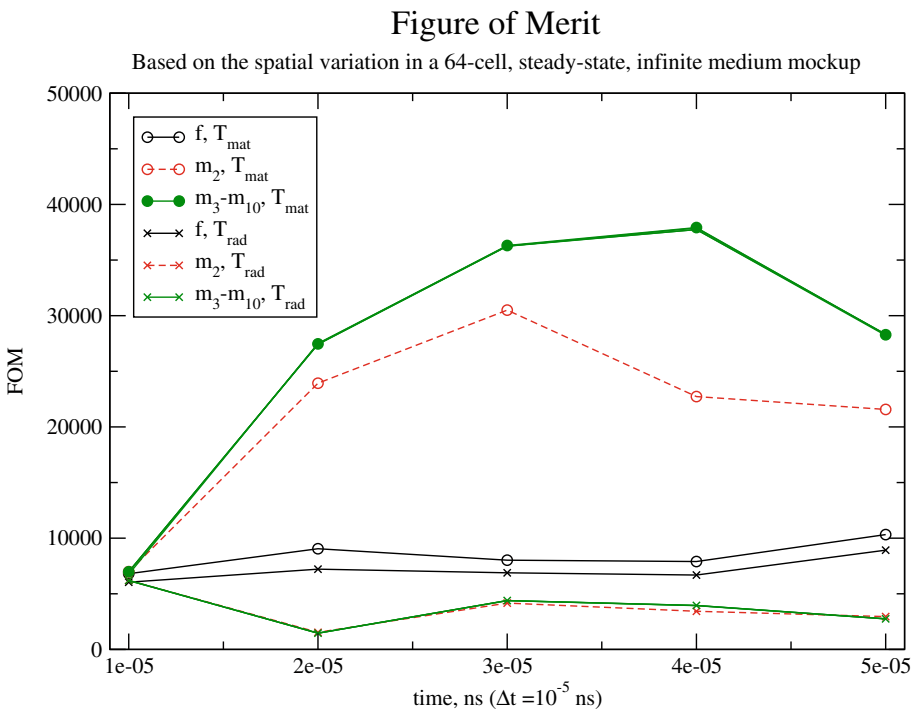

Fig. 8. merit for the radiation and material temperatures for the adaptive method and standard IMC.

where σ^2 is the variance of the estimate and t is the computer time. The computer time is proportional to the number of particles, N and, according to the Central Limit Theorem, σ^2 goes as $\mathtt{const}/N$, such that the FOM produces a nearly constant value useful for comparing the different constants associated with different methods. A larger FOM is better.

Let us consider a simple steady-state, homogeneous, infinite medium test problem in equilibrium. We model the infinite medium as a $4 \times 4 \times 4$ block of uniform cells with reflecting boundary conditions. The exact solution to this problem has the medium remaining at its initial temperature; nevertheless, a numerical solution with a Monte Carlo method and several spatial cells will induce variations about this equilibrium value. We will assume that we can use the spatial variance of the cell temperatures in our FOM calculation; the assumption of independence between the cells becomes increasingly valid as the opacity increases and the cells become more decoupled. We further assume that the opacity is inversely proportional to the material temperature to get $1000/T^3$ (T in keV), which produces a constant Fleck factor, f and a constant m_l that is unique for each value of l. The density is $3\ \mathrm{g/cm^3}$, the timestep is a constant 10^{-5} ns, the cells are $1\ \mathrm{cm^3}$ cubes and $\rho c_v = 0.1\ \mathrm{GJ/cm^3\text{-}keV}$. The run times per time step were about 25 sec for Fleck and Cummings IMC, 29.5 sec for m_2 and 30.5 sec for m_3 and above. The spatial variations of temperature over four time steps are shown in Figs. 6 and 7 for the material and radiation, respectively, for both f and m_3 (that is, where m_3 is the maximum value for our adaptive method). In each figure, the sets of points with lower variance are shown with thick lines. With m_3, the material temperature variation is less than that for standard Fleck and Cummings IMC and the radiation temperature variation increases. The resulting FOMs are shown in Fig. 8, where we see a 2 to 4 increase in the material temperature FOM and a 2 to 4 decrease in the radiation temperature FOM. In the IMC simulation for both methods, the particles undergo implicit absorption between effective scatters [17]. The radiation temperature derives from a path-length estimator of the radiation energy and the material temperature derives from an inverse heat capacity-weighted energy deposition, which derives from a path-length estimator of the particles undergoing implicit absorption. The two estimators are anti-correlated because their base tallies sum to the energy-weight path-length for each particle track. However, the driving force here is the decreased coupling between the material and radiation.

The reduction of noise in the material temperature is important even if it comes at a cost of marginally increased radiation noise. We argue that it is more important to reduce noise in the material temperature because of additional coupling concerns. In a radiation hydrodynamics simulation the material temperature couples to other physical operators including the eponymous hydrodynamics operator, equation of state calculations and perhaps atomic physics equations. These other physical operators are likely treated with deterministic methods that may be sensitive to noise in the material temperature. On the other hand, noise in the radiation field is only directly seen by the implicit Monte Carlo method, which handles noise in the solution as a matter of course.

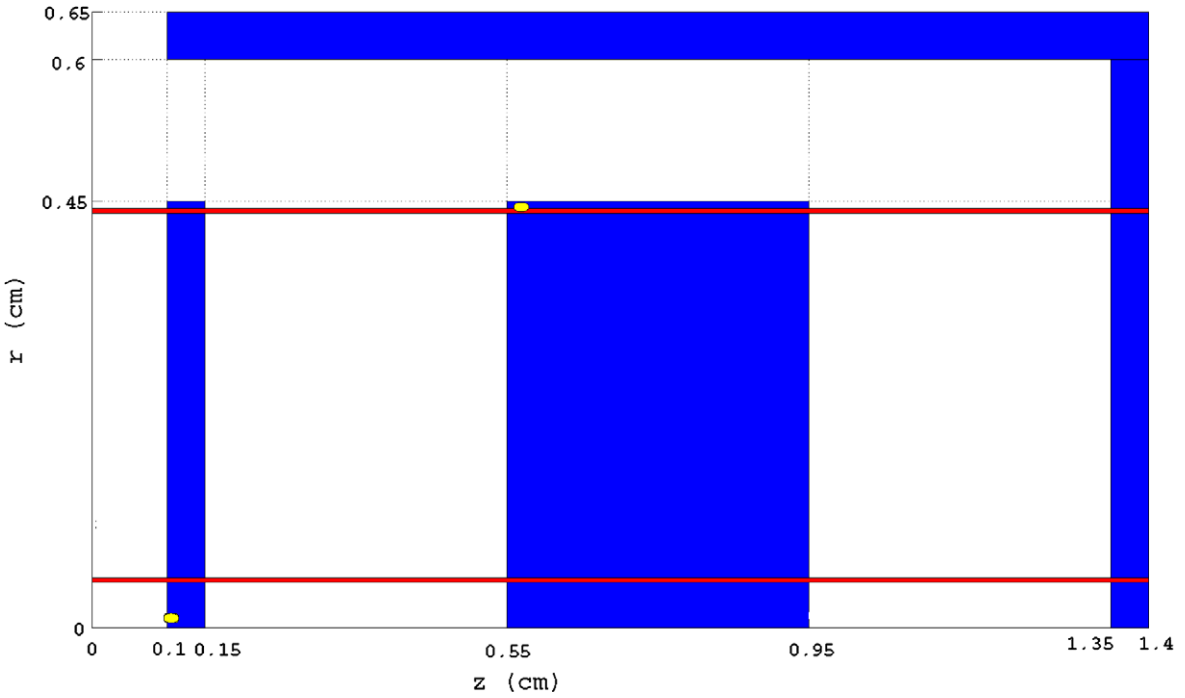

Fig. 9. Layout for the hohlraum problem: the shaded regions have $\sigma = 300T^{-3}$ cm^{-1} with T in keV, $\rho c_v = 0.3$ GJ/cm^3-keV; the white regions are vacuum. There is a 1 keV boundary source at $z = 0$ and the problem is initially cold. The lines at $r = 0.05, 0.44$ and the dots at $(r, z) = (0.005, 0.105)$ and $(0.44, 0.56)$ indicate areas were we look at the solution in detail in later figures.

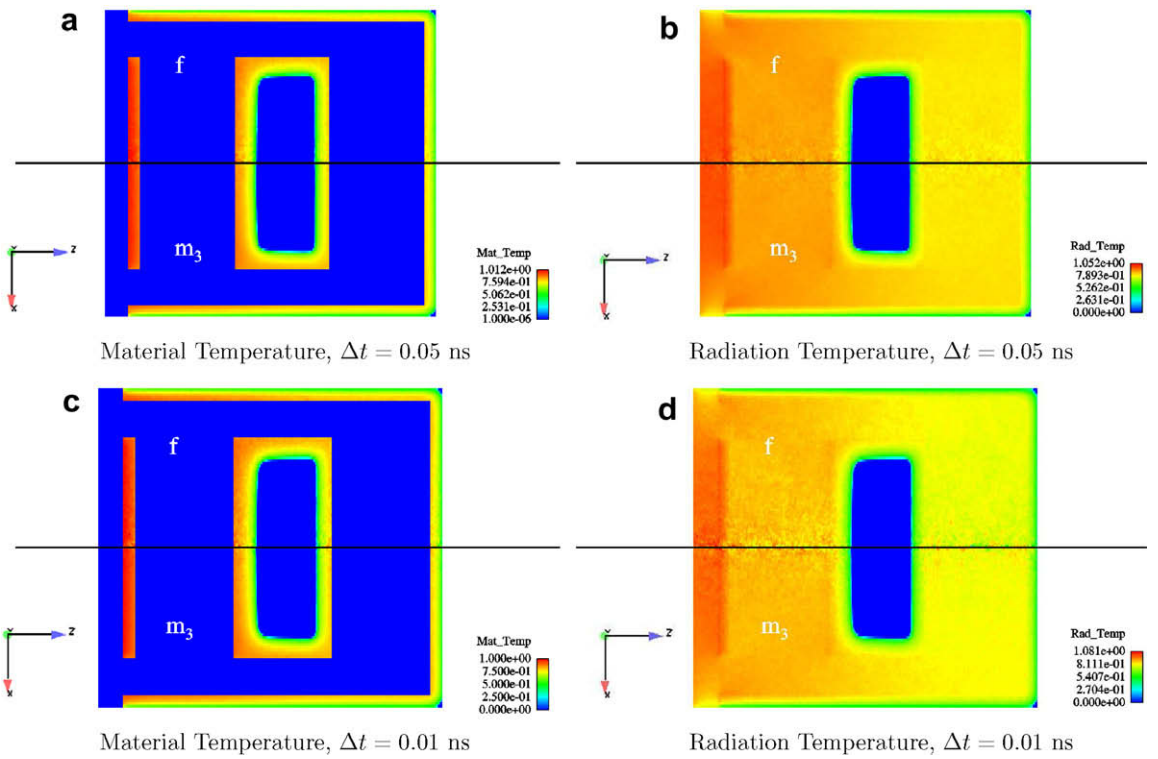

Fig. 10. Results for the hohlraum problem at $t = 10$ ns. The top and bottom halves of each subfigure are, respectively, the standard IMC solution and the adaptive solution with the maximum l set to 3.

9. Multidimensional results

To demonstrate the effectiveness of the adaptive scheme to choose the integration order l, we solve a problem relevant to inertial confinement fusion using an indirect drive, hohlraum configuration. The layout of the problem is due to Brunner [18], though we have changed the problem from planar geometry to cylindrical $r-z$ geometry. The layout of the problem is shown in Fig. 9.

In Fig. 10 we compare the solutions from standard IMC with our adaptive scheme with a maximum integration order of 3 with fixed time step sizes. All problems used 5×10^5 particles per time step initially, ramping up to 10^6 particles per time step by the end of the simulation; the computational mesh has uniform spacing of 65 cells in the r direction and 260 cells in the z direction. In Fig. 10, as well as our subsequent figures, there is noticeably less noise in the adaptive solution than in standard IMC. The reduced noise is a result of there being more effective scattering in those regions of the problem where the integration order is increased. Also, we notice that in the $\Delta t = 0.01$ ns solution the temperature wave has propagated slightly farther into the central block in the standard IMC solution.

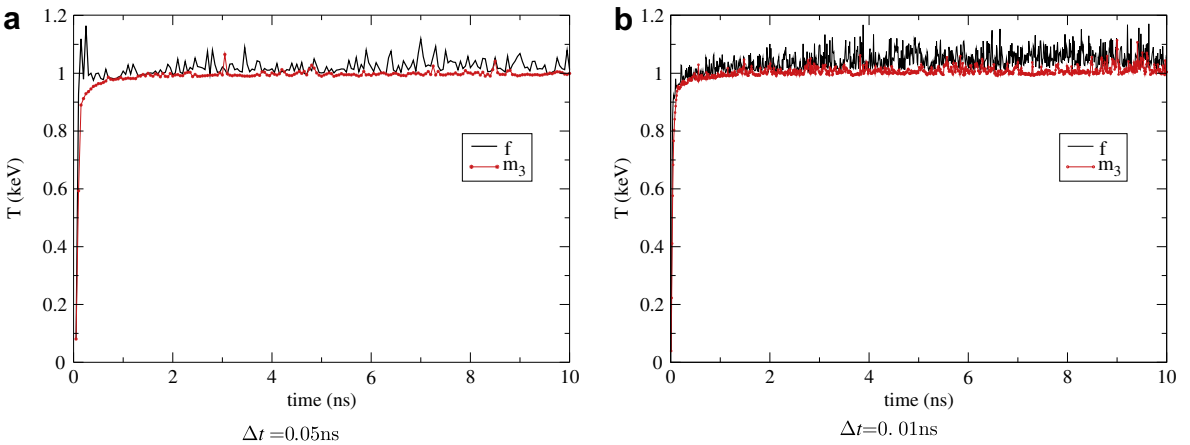

Fig. 11. Comparison of the maximum material temperature for the adaptive scheme and standard IMC.

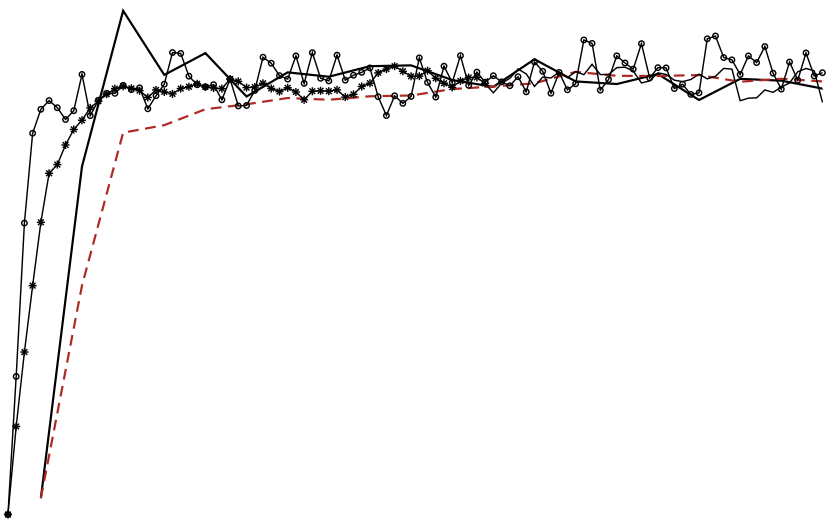

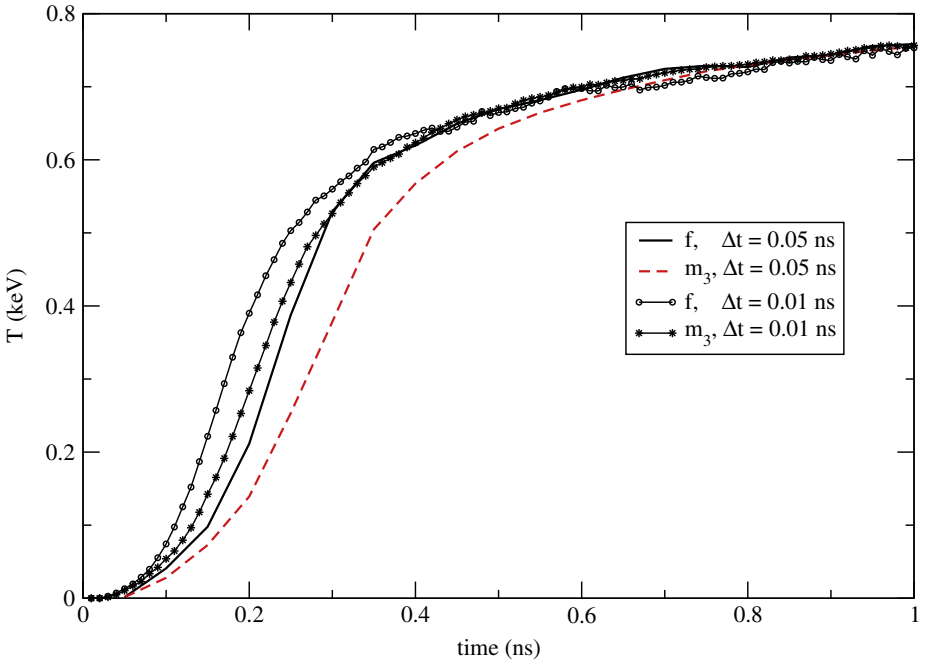

Fig. 13. The material temperature as a function of time at $(r,z) = (0.44, 0.56)$.

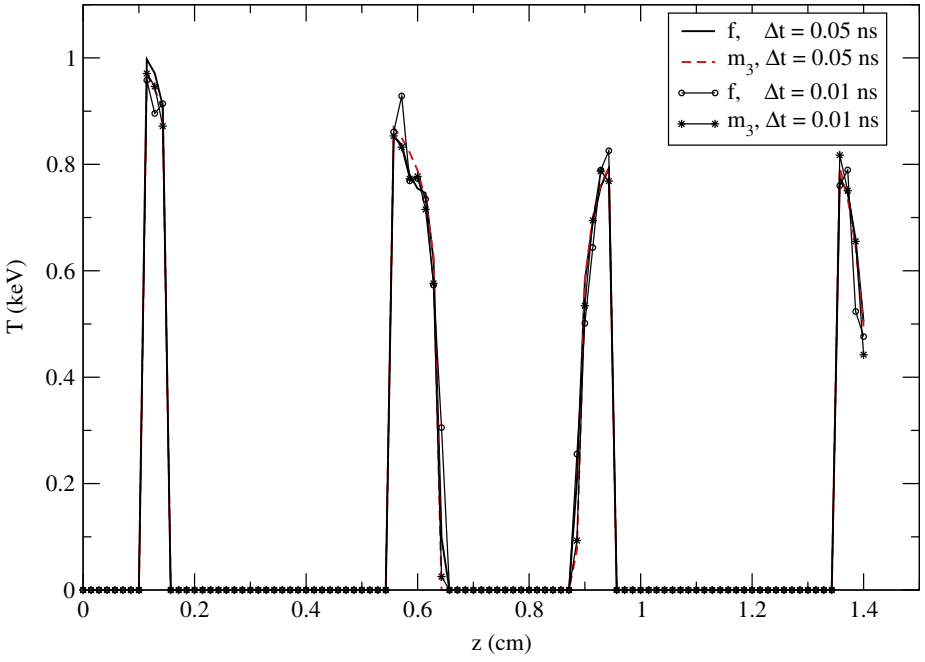

Fig. 14. The material temperature at $r = 0.05$ cm,$t = 10$ ns.

The effect of the adaptive scheme on the maximum material temperature as a function of time is shown in Fig. 11. This figure demonstrates that standard IMC has the maximum temperature above the 1 keV drive temperature for most of the problem. The adaptive scheme does not completely eliminate this overheating, but the maximum temperatures with the adaptive scheme are smaller than standard IMC.

The differences in the initial heating transient are demonstrated in Figs. 12 and 13 by the plots of the temperature as a function of time at the fiducial points. At $(r,z) = (0.005, 0.105)$, a point that is directly irradiated by the boundary source, the

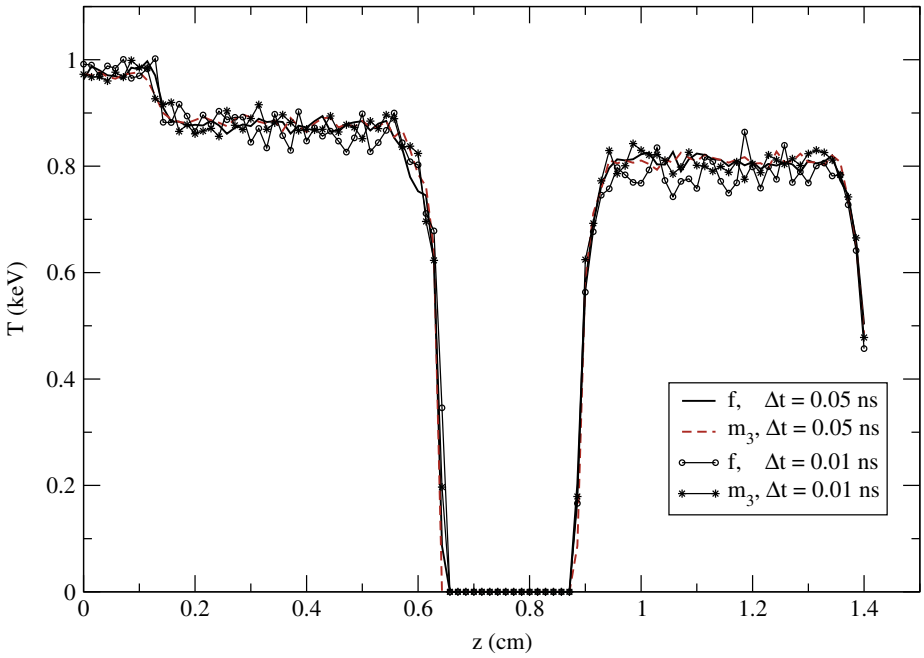

Fig. 15. The radiation temperature at $r = 0.05$ cm,$t = 10$ ns.

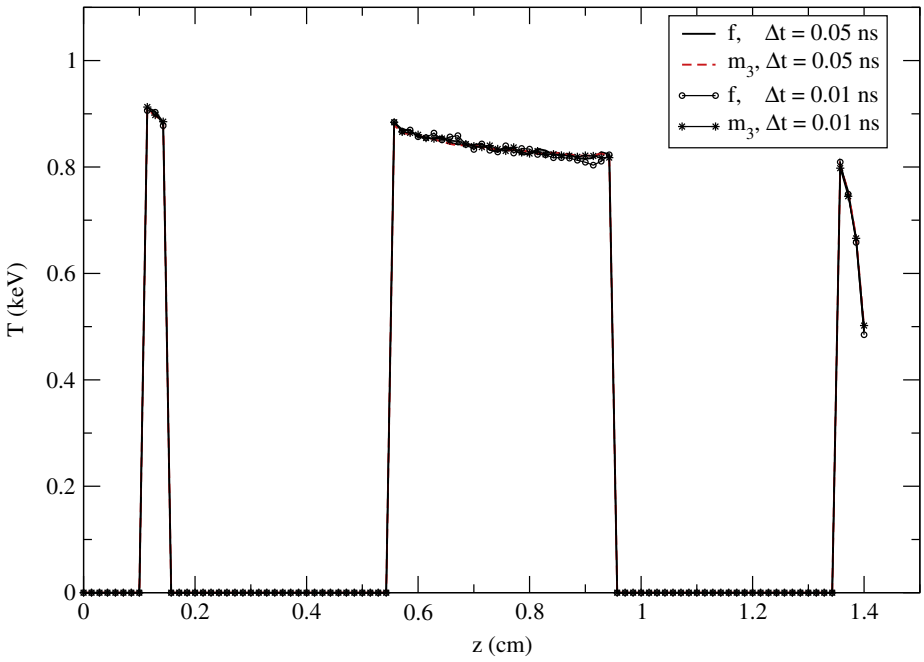

Fig. 16. The material temperature at $r = 0.44$ cm, $t = 10$ ns.

standard IMC solution overshoots the drive temperature in its early transient. The adaptive scheme solution has a monotonic transient, with both sizes of time step. At the point $(r, z) = (0.44, 0.56)$ the transient from 0 to 1 ns has the same behavior for the different methods but different rise times. The adaptive scheme's results heat up more slowly than standard IMC for a given time step. We do note that in terms of the entire solution time, this slight change in transient behavior is a minor effect. Outside the transient region all methods converge to the same temperature at these two points.

Turning to geometric comparisons of the solutions, Figs. 14 and 15 show the material and radiation temperatures at $t = 10$ ns and $r = 0.005$ cm. The material temperatures in Fig. 14 are in general agreement between the two methods. The

largest discrepancy is near $r = 0.6$ cm with the standard IMC solution and $\Delta t = 0.01$ ns. This could be attributed to solution noise. The radiation temperature solutions are also mostly in agreement, although the small time step solution with standard IMC is plagued by noise. Along the line at $r = 0.44$ cm the material temperatures are in general agreement across all solutions (c.f. Fig. 16).

As we pointed out in the previous section, the solutions produced by the adaptive method have less noise in the material temperature than the standard IMC results. In our figures of merit we saw that the decreased noise in the material came at a cost of increased noise in the radiation. In the hohlraum problem there is clearly a reduction the noise in the material temperature and the noise in the radiation solution did not increase noticeably. This is likely a result of the large regions of vacuum in this problem: the material temperature of the walls directly couples to the radiation in the vacuum regions. Therefore, the reduction of noise in the material temperature can lead to a reduction of noise in the radiation temperature in the vacuum regions.

10. Conclusions

We have presented a new implicit Monte Carlo method, in both grey and multifrequency situations, that provides a framework to suppress the nonphysical overheating that can occur in the standard Fleck and Cummings IMC method when large time steps are used. The method we have presented has the same properties in the diffusion limit as standard IMC. In its implementation this new method differs from Fleck and Cummings IMC method only in the changing of the f factor to an adaptively selected m_l factor.

Infinite medium numerical results demonstrated how the choice of the integration order, l, affects the amount of heating as a function of time. Where standard IMC nonphysically overheated the material and then had the material temperature oscillate around the equilibrium temperature, the modified IMC solutions with the Fleck factor replaced by m_l approached the equilibrium temperature monotonically. For large initial differences in the radiation and material temperatures, the m_l solution did overshoot the equilibrium temperature for $l = 3$.

Inspired by the infinite medium results, we developed an adaptive scheme to suppress the overheating that can be present in standard IMC. The adaptivity is based on solving a 0-D problem in each computational cell; where the solution to the 0-D problem indicates that overheating could occur, we adjust the integration order to prevent the overheating. Using the adaptive method on a multi-celled infinite medium problem, figures of merit indicated that the adaptive method suppresses noise in the material temperature, but increased noise in the radiation temperature.

On a multidimensional problem, we showed that using the adaptive method suppressed most of the overheating that was found in the standard IMC solution. Moreover, the adaptive solutions had less noise than standard IMC for the same number of particles, an effect due to the added scattering in the problem. Though the behavior in transients was changed and the amount of noise differed, both the adaptive scheme and standard IMC gave solutions that were mostly in agreement at late times. In this problem the noise in the material temperature decreased and there was no noticeable increase in the radiation temperature noise.

In the future we will investigate combining our method with semi-implicit ideas of Gentile [7] that include the variation of the opacity with temperature in the linearization. Including the opacity in the linearization is compatible with our method and should enhance the method's robustness. We also plan on exploring the idea of solving a 0-D problem in each cell to prescribe a time step control rather than changing the integration order. Beyond these extensions we hope to apply our method to radiation hydrodynamics simulations of astrophysical phenomena and internal confinement fusion.

Acknowledgments

The authors would like to thank J.D. Densmore for several conversations during our development of this work. Also, the anonymous reviewers provided suggestions that improved the presentation and clarity of our manuscript.

Portions of this work were performed under U.S. government contract DE-AC52-06NA25396 for Los Alamos National Laboratory, which is operated by Los Alamos National Security, LLC. (LANS) for the U.S. Department of Energy LA-UR-09-02297.

References

[1] J.A. Fleck Jr., J.D. Cummings, An implicit Monte Carlo scheme for calculating time and frequency dependent nonlinear radiation transport, J. Comp. Phys. 8 (1971) 313–342.
[2] E.W. Larsen, B. Mercier, Analysis of Monte Carlo method for nonlinear radiative transfer, J. Comp. Phys. 71 (1987) 50–64.
[3] E.S. Andreev, M.Y. Kozmanov, E.B. Rachilov, Maximum principle for a system of equations of energy and non-stationary radiation transfer, U.S.S.R. Comput. Math. Math. Phys. 23 (1983) 104.
[4] B. Mercier, Application of accretive operators theory to the radiative transfer equations, SIAM J. Math. Anal. 18 (2) (1987) 393–408.
[5] S.W. Mosher, J.D. Densmore, Stability and monotonicity conditions for linear, grey, 0-D implicit Monte Carlo calculations, Trans. Am. Nuc. Soc. 93 (2005) 520.
[6] J.D. Densmore, E.W. Larsen, Asymptotic equilibrium diffusion analysis of time-dependent Monte Carlo methods for gray radiative transfer, J. Comp. Phys. 199 (2004) 175–204.
[7] N.A. Gentile, A comparison of various temporal discretization schemes for infinite media radiation transport, Trans. Am. Nuc. Soc. 97 (2007) 544.
[8] L.L. Carter, C.A. Forest, Nonlinear radiation transport simulation with an implicit Monte Carlo method, Tech. Rep. LA-5038, Los Alamos National Laboratory, 1973.
[9] E.D. Brooks III, Symbolic implicit Monte Carlo, J. Comp. Phys. 83 (1989) 433.

[10] T. N'kaoua, Solution of the nonlinear radiative transfer equations by a fully implicit matrix Monte Carlo method coupled with the Rosseland diffusion equation via domain decomposition, SIAM J. Sci. Stat. Comput. 12 (1991) 505.
[11] A.B. Wollaber, Advanced Monte Carlo Methods for Thermal Radiation Transport, Ph.D. Thesis, University of Michigan, Ann Arbor, 2008.
[12] K. Dekker, J.G. Verwer, Stability of Runge-Kutta Methods for Stiff Nonlinear Differential Equations, Elsevier, North Holland, Amsterdam, 1984.
[13] E.W. Larsen, G.C. Pomraning, V.C. Badham, Asymptotic analysis of radiative transfer problems, J. Quant. Spec. Rad. Transf. 29 (4) (1983) 285–310.
[14] S.W. Mosher, Exact solution of a nonlinear, time-dependent, infinite-medium, grey radiative transfer problem, Trans. Am. Nucl. Soc. 95 (2006) 744–747.
[15] N.A. Gentile, Personal communication, December 2007.
[16] J.F. Briesmeister, MCNP-A General Monte Carlo N-Particle Transport Code, No. LA-12625-M, Version 4B, Los Alamos National Laboratory, 1997.
[17] T.J. Urbatsch, T.M. Evans, Milagro version 2, an implicit Monte Carlo code for thermal radiative transfer: Capabilities, development and usage, Tech. Rep. LA-14195-MS, Los Alamos National Laboratory, January 2005.
[18] T.A. Brunner, Forms of approximate radiation transport, Tech. Rep. SAND2002-1778, Sandia National Laboratories, July 2002.